



Proceedings of the Seventeenth International Conference on  
Civil, Structural and Environmental Engineering Computing  
Edited by: P. Iványi, J. Kruis and B.H.V. Topping  
Civil-Comp Conferences, Volume 6, Paper 1.1  
Civil-Comp Press, Edinburgh, United Kingdom, 2023  
doi: 10.4203/ccc.6.1.1  
©Civil-Comp Ltd, Edinburgh, UK, 2023

# Advances in Computational Constitutive Modeling

L. Moreno<sup>1</sup>, L. Saucedo<sup>1</sup>, M.A. Sáenz<sup>1</sup> and F.J. Montáns<sup>1,2</sup>

<sup>1</sup>Universidad Politécnica de Madrid  
Madrid, Spain

<sup>2</sup>University of Florida  
Gainesville, Florida, United States of America

## Abstract

Constitutive models are a key ingredient of finite element procedures. Robust and efficient finite element solutions require sound physically motivated multiaxial models that, at the same time, are simple, efficient and as general as possible. Furthermore, material parameters should be reduced to a minimum and, if possible, either obtained directly from experimental measurements or obtained through automatic procedures. In this paper we overview recent advances in large strain constitutive models following these principles. In the first part, we address the main ideas behind a new class of hyperelastic models which parameters can be automatically obtained from experimental measurements. In the second part we address a new class of constitutive models for multiaxial, anisotropic viscoelasticity and plasticity, which is based on the elastic corrector rate concept, and whose algorithms result in plain backward-Euler updates. These formulations also bring an identical framework in both continuum and crystal plasticity.

**Keywords:** hyperelasticity, polymers, soft materials, plasticity, viscoelasticity, crystal plasticity

# 1 Introduction

The modeling of deformable components using finite elements need reliable finite element formulations and sound, efficient and robust constitutive models and algorithms [1]. Bathe et al. [2] established the equivalency between the widely used large strain Updated Lagrangean and Total Lagrangean finite element approaches, and constitutive models have been mainly confined to material subroutines which relate stresses to the deformation gradient; hyperelasticity was already therein considered. But despite hyperelasticity had been around for decades in physics, chemistry and applied mathematics to model rubber-like materials (see e.g. [3,4] and therein references), it was probably Simo and coworkers who made the important leap of promoting hyperelasticity not just as a material modeling approach for soft materials, but as a requirement also in metals to avoid spurious dissipation both at the constitutive and the algorithmic levels [5], avoiding ad-hoc “objective” integration rules and prescribing a physically correct behaviour by construction. Through rigorous treatments, Simo and coworkers also derived the algorithmically consistent tangent in elastoplasticity and the large strain formulations based on the Kröner-Lee multiplicative decomposition. This energy-based combination, avoiding theoretical shortcuts as hypoelastic rate-form evolution equations or plastic “metrics”, resulted not only in sound theories, but also in remarkably simpler algorithmic treatments. This presentation is framed in these ideas: using sound theoretical modeling to arrive at simpler computational procedures. We present the recent advances made in our group in the last years in constitutive modeling.

In the first part we shortly overview a new approach to model soft materials. Our work is based on the seminal ideas from Sussman and Bathe [6] of using spline-based interpolation to yield a non-parametric approach to hyperelasticity. We have extended this approach to model soft materials [7–12] both from a phenomenological point of view and from a micromechanical point of view. We have determined the spline coefficients both from homogeneous tests on the material and from finite element results on nonhomogeneous tests, in both cases just solving a linear system of equations. With this procedure we have also been able to obtain important physical insight in the theory of polymers [13, 14].

In the second part, we introduce the basic ideas and advantages of a new class of large strain formulations for plasticity and viscoelasticity based on the concept of elastic corrector rates [15–18]. This new approach overcomes many of the problems and limitations encountered in more classical multiplicative large strain plasticity formulations. For instance, the new approach is (1) valid for arbitrarily large elastic or plastic deformations, (2) has uncoupled plastic spin, (3) the Madel tensor is irrelevant also in anisotropic formulations and (4) it is integrated using a simplest *plain* backward-Euler integration rule, preserving the isochoric behavior by construction. It also allows for strain-level dependent viscoelasticity without the use of Prony series or strain-dependent parameters [19]. This framework has been extended to model nonlinear kinematic hardening at large strains using only the Lee decomposition [20] and to model crystal plasticity [21].

## 2 A new succesful approach to hyperelasticity

In this section we overview the novel approach to hyperelassticity using spline interpolations, and how this data-driven method brought a new non-affine micro-macro connection which solves many of the interrogants in the modeling of elastomers.

### 2.1 Spline-based hyperelasticity

Hyperelasticity is true path-independent, conservative elasticity. An elastic model has to fulfill Bernstein's integrability conditions to avoid spurious energy disipation during closed cycles [22, 23]. This is guaranteed through the assumption of an energy potential (the hyperelastic model), whose strain derivatives are the stresses. The main drawback is that stored energies cannot be measured, so their shapes are "guessed", as a function of some material parameters that are adjusted fitting stress-strain data for some loading protocols. Well known hyperelastic models are the Ogden model, the Arruda-Boyce model, the Mooney-Rivlin model, etc. [1, 4].

Sussman and Bathe [6] brought a new paradigm to hyperelasticity using splines to describe the stored energy function. Splines are series of local cubic polynomia which coefficients (the "parameters") in the stored energy can be easily manipulated and brought to the stress-strain curve. Then, they can be obtained automatically simply solving the linear system of equations which results from the minimization of the squared error. They are considered "non-parametric" because these coefficients are never "seen" by the user. In some sense, the method is similar to Neural Networks (in being non-parametric), but the latter (also used in hyperelasticity) do not preserve any physical insight. It is also similar to finite elements in the sense that local interpolations are employed and the nodal values are obtained from equilibrium.

The simplest case is that of isotropic incompressible materials based on the Valanis-Landel decomposition. In this case, if we use logarithmic strains  $E_i = \ln \lambda_i$ , where  $\lambda_i$  are the stretches, the stored energy function  $\Psi$  may be written as

$$\Psi(E_1, E_2, E_3) = \omega(E_1) + \omega(E_2) + \omega(E_3) \quad (1)$$

We can posit that each Valanis-Landel term (indeed its derivative) can be written in terms of spline interpolation functions  $N_i(\xi(E))$  as

$$\omega'(E) = \sum_{i=1}^{nv} N_i(\xi(E)) \hat{\omega}_i \quad (2)$$

where  $\hat{\omega}_i = \omega'(E_i) - \omega'(0)$  are the "nodal" values (vertices in B-splines) to be determined,  $\xi(E)$  is the normalized domain variable, and  $nv$  is thenumber of functions/vertices used.

In the Valanis-Landel case, the equilibrium equation for a uniaxial test is

$$\sigma_u(E_u) = \left. \frac{\omega(E)}{dE} \right|_{E=E_u} - \left. \frac{\omega(E)}{dE} \right|_{E=-\frac{1}{2}E_u} \Rightarrow \sigma_u(E) = \omega'(E) - \omega'(-\frac{1}{2}E) \quad (3)$$

where the second expression is a compact notation. Eq. (3) can be evaluated at every experimental value  $E_i$ , so using the interpolation Eq. (2), a system of equations may be formed, from which the nodal values  $\hat{\omega}_i$  may be obtained. In practice, less vertices than experimental data are used, so a minimizing solution for the squared error is pursued, using the Moore-Penrose Pseudoinverse.

Whereas initial works used cubic splines, penalized B-splines are a much better choice because of two reasons: convexity of the energy can be guaranteed by guaranteeing the convexity of the hull of the B-spline vertices, and smoothing penalization is straightforward [24]

Whereas the previous explanation is for isotropic materials, the approach is equally valid for anisotropic materials. The main changes are the assumption on the main invariants to be used and the assumption of the strain energy decomposition. Some cases may even be strikingly simple. If we assume that the stored energy may be written as (an assumption common to many models, for example the Holzapfel-Gasser-Ogden model)

$$\Psi = \psi_{iso}(I_1) + \psi(I_4) + \psi(I_6) \quad \text{with } I_1 = \text{trace}(\mathbf{C}), I_i = \mathbf{C} : \mathbf{a}_i \otimes \mathbf{a}_i, i = 4, 6 \quad (4)$$

where  $\mathbf{a}_i$  are the fiber directions,  $\mathbf{C}$  is the right Cauchy-Green deformation tensor and  $I_i$  the related invariants, then *the stored energy solution is explicit from a tensile test data* [25]:

$$\psi'_{iso}(I_1) = \frac{\frac{1}{2}(1 - \cos 2\beta)\lambda_t^2 \sigma_u}{2\lambda_t^2(\lambda_u^2 - \lambda_3^2) \sin^2 \beta - 2\lambda_u^2(\lambda_t^2 - \lambda_3^2) \cos^2 \beta} \quad (5)$$

$$\psi'(I_u) = \frac{\frac{1}{2}(\lambda_3^2 - \lambda_t^2)\sigma_u}{2\lambda_t^2(\lambda_u^2 - \lambda_3^2) \sin^2 \beta - 2\lambda_u^2(\lambda_t^2 - \lambda_3^2) \cos^2 \beta} \quad (6)$$

Here  $\beta$  is the angle between fibers ( $\beta/2$  is the angle with the loading direction),  $I_u = I_4 = I_6 = \lambda_u^2 \cos^2 \beta + \lambda_t^2 \sin^2 \beta$  is the anisotropic invariant,  $\lambda_u, \lambda_t$  are the longitudinal and transverse stretches in the uniaxial test, and  $\sigma_u$  are the stresses. Hence, remarkably, with Eqs. (5), (6), we do *not* need to prescribe the shape or “model” of the stored energy, (less determine any material parameter as in the HGO model). We just interpolate nodal values!

One of the most important works in this line is the determination of the behavior of a representative elastomer chain from tests on the continuum. In this case, we assume that the polymer is made of macromolecules randomly oriented in space. Their entropy changes with stretch. We assume that the stored energy of the solid can be computed from integration in all directions of space (in the sphere  $S$ ); that is:

$$\Psi(\lambda_1, \lambda_2, \lambda_3) = \frac{1}{S} \int_S \Psi_{ch}(\lambda_{ch}) dS \quad (7)$$

The stresses are determined from the stretch-derivatives of this stored energy

$$\frac{\partial \Psi(\lambda_1, \lambda_2, \lambda_3)}{\partial \lambda_i} = \frac{1}{S} \int_S \frac{d\Psi_{ch}(\lambda_{ch})}{d\lambda_{ch}} \frac{\partial \lambda_{ch}}{\partial \lambda_i} dS \quad (8)$$

We can use B-spline interpolations to describe the derivative of the chain function  $P_{ch} := d\Psi_{ch}(\lambda_{ch})/d\lambda_{ch}$ :

$$P_{ch} = \sum_{m=1}^{nv} N_m(\lambda_{ch}(\lambda_1, \lambda_2, \lambda_3, \mathbf{r}_{ch})) \hat{P}_{ch_m} \quad (9)$$

where  $nv$  is the number of the B-spline vertices,  $\mathbf{r}_{ch}$  is the direction of the specific chain and  $\lambda_{ch}(\lambda_1, \lambda_2, \lambda_3, \mathbf{r}_{ch})$  is a function of the continuum stretches and the chain direction. Inserting this interpolation into Eq. (8), after some algebra (see [14]), we arrive to a linear system of equations, which, using stress-strain data of any test, gives the vertices of the spline representing the chain behavior. With that chain behavior, using again Eq. (8), we can obtain the stress under any loading condition.

This model has been extremely succesful. It has been the first model capable of obtaining accurately all the curves (both axes) of the true biaxial Kawabata tests using only data from a single test. The results can be seen in Figure 1; see [14].

The approach can be extended to cross scales, so the representative polymer chain behavior may be obtained directly from Digital Image Correlation on non-homogeneous tests, again solving a linear system of equations. Figure 2 shows the results of simulations of a perforated plate of isoprene rubber vulcanizate when the macromolecule entropy changes are obtained directly from deformations on a nonhomogeneous test and the force applied to the specimen. Details can be found in [27].

## 2.2 Non-affine microstrech deformations

Interestingly, one of the main contradictions in the classical models of elastomers is the need for more than one test curve to characterize the material [28,29]. Note that in the linear elastic case, an isotropic incompressible material has only one independent material constant, the shear modulus, so one expects that the nonlinear case should be fully characterized by a single stress-strain curve, for example, from a uniaxial test. Equation (8) may seem an obvious exercise of the chain rule, but it is extremely important. The dependency of the microstretch  $\lambda_{ch}$  on the principal stretches  $\lambda_i$  is the micro-macro connection, and this relation is crucial. Thanks to the new approach, we have demonstrated in [13] that the classical orientational affine connection given by  $\lambda_{ch}^C = \mathbf{C} : \mathbf{r}_{ch} \otimes \mathbf{r}_{ch}$  is *not* capable of reproducing adequately the elastomer behavior (e.g. Kawabata tests) regardless of any possible chain function being used. Moreover, we have also demonstrated that the micro-macro connection  $\lambda_{ch} = \mathbf{U} : \mathbf{r}_{ch} \otimes \mathbf{r}_{ch}$  brings accurate results and is the one consistent with the statistical theory of polymers. In fact, this new micro-macro orientationally non-affine connection solves many of the inconsistencies highlighted by researchers for decades, for example: “In contrast to the original success of the statistical theory, the failure to secure any very significant understanding of the relatively rather small (?) deviations from the theory, despite repeated attempts over a period of 30 years, is disappointing”, Treloar [3] in 1975, regarding the unexplained slope in Mooney plots. Other statements are: It is “somewhat surprising the lack of success of the full network model” (e.g. Eq. (8));

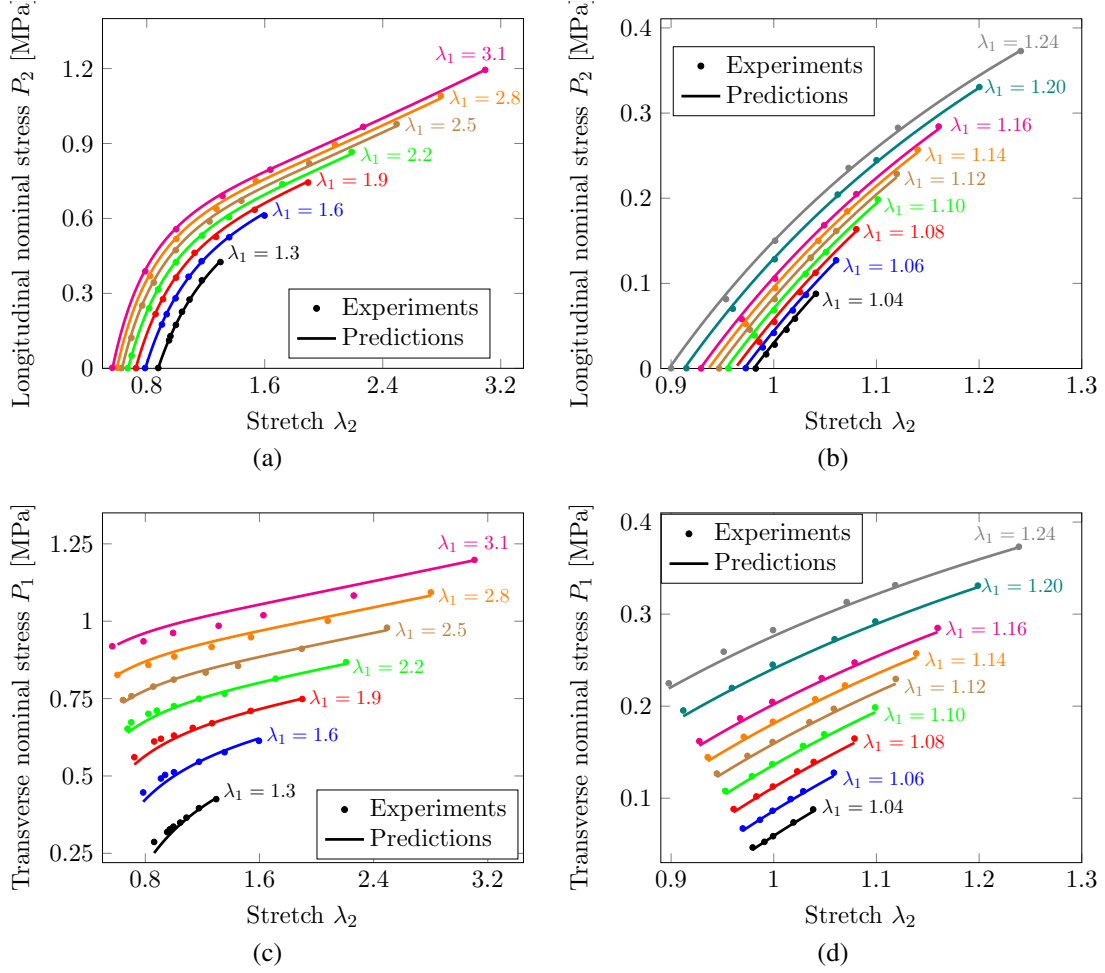


Figure 1: Predictions of the Kawabata et al biaxial experiments [26] using the proposed spline-based model. (a), (b) Longitudinal nominal stresses  $P_2$  as a function of the longitudinal stretch  $\lambda_2$  for different fixed values of the transverse stretch  $\lambda_1$ . (a) shows the large stretches range and (b) shows the moderate stretches range. (c), (d) Transverse nominal stresses  $P_1$  as a function of the longitudinal stretch  $\lambda_2$  for different fixed values of the transverse stretch  $\lambda_1$ . (c) shows the large stretches range and (d) shows the moderate stretches range. Reproduced from [14], under permission.

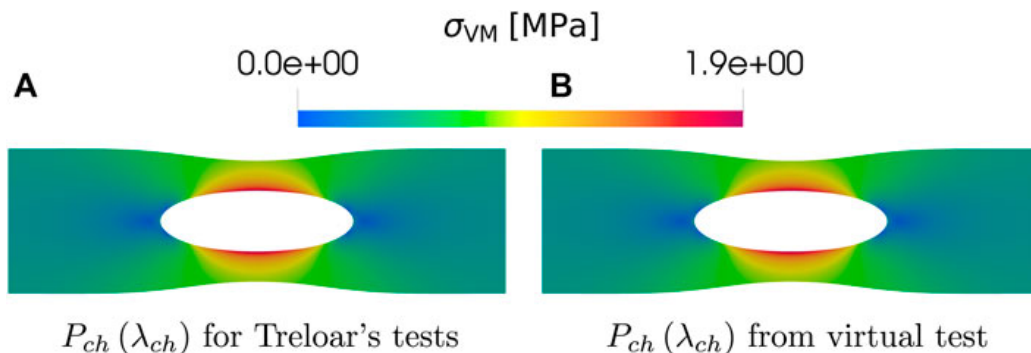


Figure 2: Comparison of the von Mises stress of a simulation of a plate with a hole made of Treloar’s rubber, when (A) the chain behavior has been obtained from homogeneous tests and (B) when they have been obtained directly from nonhomogeneous tests (in this case Digital Image Correlation measurements have been simulated through a virtual test). Reproduced from [27].

“It is a well-known fact that the [chain stretch] affinity assumption yields a model response that is not in agreement with experimental data”, Miehe [30] regarding the need for using his proposal of the type  $\langle \lambda \rangle_q = [\int_S (\lambda_{ch}^C)^q dS/S]^{1/q}$  (note that this non-affinity relates to the stretch amount, not to the orientation of the chains, which remain affine); “It is now well-established that a unique experiment is not sufficient to characterize a [isotropic and incompressible] rubber-like material even assuming it is elastic”, [31].

With the orientationally non-affine micro-macro connection, the slope in the Mooney plots is correctly predicted, the full network model is accurate, the chain stretch needs not to be modified, and a unique (any) stress-strain curve is sufficient to fully characterize the behavior of the polymer. Indeed, just three parameters obtained from that test are sufficient [32].

### 3 Plasticity and viscoelasticity based on the notion of an elastic corrector rate

Classical large strain plasticity and viscoelasticity frameworks, based on objective stress measures and rate equations have been surpassed by schemes based on the multiplicative decomposition of the deformation gradient, the Lee decomposition for plasticity and the Sidoroff decomposition for viscoelasticity:

$$\mathbf{X} = \mathbf{X}_e \mathbf{X}_p \text{ for plasticity, or } \mathbf{X} = \mathbf{X}_e \mathbf{X}_v \text{ for viscoelasticity} \quad (10)$$

$\mathbf{X}$  is the deformation gradient [1] and subscripts stand for elastic, plastic or viscous contributions. This decomposition, motivated in crystal plasticity, allowed for the use of hyperelastic stored energy functions  $\Psi(\mathbf{X}_e)$ , and hence, simplified integration algo-

rithms avoiding objectivity issues. However, stress integration becomes conceptually more complex [5],

One of the main difficulties in these formulations has been the establishment of the plastic flow evolution equation. First algorithmic formulations lacked preservation of the isochoric nature of the plastic flow [5]. While this was soon solved, the algorithms remained relatively complex. The seminal works of Weber and Anand [33] and Eterović and Bathe [34] brought simplicity by the use of logarithmic strains and the so-called exponential formula. This type of formulation has been advocated later by many authors, even though some limitations remained, as the use of “moderately large” elastic strains and linear elastic relationships. Anisotropy had also many issues, due to the lack of commutation between the stress and strain tensors, bringing the non-symmetric Mandel stress tensor (of elusive interpretation). The key point to these formulations has been the use of the plastic flow evolution equation, namely

$$\mathbf{L}_p = \dot{\mathbf{X}}_p \mathbf{X}_p^{-1} \quad (11)$$

where  $\mathbf{L}_p$  is the plastic velocity gradient. However, this “phenomenological” proposal, motivated in the classical small strain setting, is the source of both the theoretical and algorithm problems. A rigorous approach establishes the logarithmic elastic strains  $\mathbf{E}_e$  as a function of the total deformation gradient  $\mathbf{X}$  and the plastic deformation gradient  $\mathbf{X}_p$  as  $\mathbf{E}_e(\mathbf{X}, \mathbf{X}_p)$ , so its rate is split into two contributions or partial derivatives

$$\dot{\mathbf{E}}_e = \left. \frac{\partial \mathbf{E}_e}{\partial \mathbf{X}} \right|_{\dot{\mathbf{X}}_p=0} : \dot{\mathbf{X}} + \left. \frac{\partial \mathbf{E}_e}{\partial \mathbf{X}_p} \right|_{\dot{\mathbf{X}}=0} : \dot{\mathbf{X}}_p =: {}^{tr} \dot{\mathbf{E}}_e + {}^{ct} \dot{\mathbf{E}}_e \quad (12)$$

The latter identity renames, for convenience, the contributions as “trial” and “corrector” contributions, because of obvious parallelism with the predictor-corrector algorithmic concepts, *but note that here we deal with continuum concepts, partial derivatives, not algorithmic concepts*. Then, it can be shown that the plastic dissipation equation and the evolution equations may be fully written in terms of the logarithmic elastic strain corrector rates, and of the work-conjugate generalized Kirchhoff stresses  $\mathbf{T}$  i.e.

$$\mathcal{D}^p = -\mathbf{T} : {}^{ct} \dot{\mathbf{E}}_e \geq 0 \quad \text{with} \quad {}^{ct} \dot{\mathbf{E}}_e = -\dot{\gamma} \nabla \phi / k \quad (13)$$

where  $\dot{\gamma}$ , is the effective plastic deformation rate,  $k$  is the equivalent yield stress and  $\phi$  is the flow potential (e.g. the derivative of the yield surface respect to the stresses).

Thanks to this approach, when using also logarithmic strains in the intermediate configuration, the stress integration algorithm is a simple backward-Euler algorithm, and no restriction on the hyperelastic relations or the magnitude of the elastic strains is needed. Anisotropy is incorporated in a straightforward manner. Indeed, the motivation and first implementation was using Hill plasticity [16]. Furthermore, the Mandel stress plays no role in the formulation and no assumption regarding the plastic spin is needed (because it is uncoupled from the symmetric flow).

Using Prandtl elements in series, this type of formulation has been extended to model nonlinear kinematic hardening at large strains using only Lee multiplicative

decompositions (avoiding Lion-type decompositions), and avoiding spurious energy dissipation due to backstress integration [20]. Indeed, even the concept of backstress is nonexistent in the new formulation. In Fig. 3 we show the simulation of a cyclic bending test on a plate using rollers. It is seen in the figure that nonlinear kinematic hardening is correctly reproduced (including Masing rules), and no spurious dissipation is apparent. The formulation is robust, capable of simulating the strong changes due to contact conditions.

The framework based on elastic corrector rates has also been extended to crystal plasticity, where all the attractive properties are preserved, and a complete parallelism between continuum and crystal plasticity formulations is obtained. Among the attractive properties is the use of any hyperelastic function, the absence of the Mandel stress tensor, the plain backward-Euler integration rule, and the fulfillment of the weak-invariance properties [21]. Interestingly, using equivalent material parameters, the computational results are in close agreement with those from the classical (more complex) Kalidindi-Bronkhorst-Anand formulation. Figure 4 shows the simulation of a tensile test on a polycrystal cubic sample. Fig. 4b gives the initial crystallographic texture pole plots for directions (111) and (100) and Fig. 4c shows the final texture plots for the same directions. It can be shown that these results are visually almost indistinguishable from those obtained using the classical formulation; see details in [21].

## 4 Concluding remarks

The objective of this presentation has been to give an overview of new approaches in constitutive modeling which bring simple computational methods from minimal assumptions.

Spline-based hyperelasticity is a non-parametric data-driven method that avoids the assumption of the form of the stored energy. The only assumption is about the structure of the model, as invariants, and how the stored energy is obtained from partial energy contributions. This approach has brought a new micro-macro connection for the chain stretch that results in very accurate predictions for elastomers using a single test curve to characterize them. Furthermore, it has solved many crucial issues regarding polymer modeling that remained unsolved for decades.

In multiplicative plasticity, the formulation of the plastic flow in terms of the elastic strain corrector rate (a continuum concept) is not only mathematically and physically sound (e.g. fulfilling the weak-invariance property), but also results in simplest backward-Euler algorithms. Furthermore, the approach, almost unchanged, has been easily extended to model nonlinear kinematic hardening (without the backstress concept) and crystal plasticity (using any hyperelastic stored energy function and without the appearance of the Mandel stress tensor).

Research is still needed to extend these ideas for different classes of materials, like porous metals or many types of soft biological tissues. Research is also ongoing to extend these types of formulations to growth and remodeling, as well as viscoplasticity.

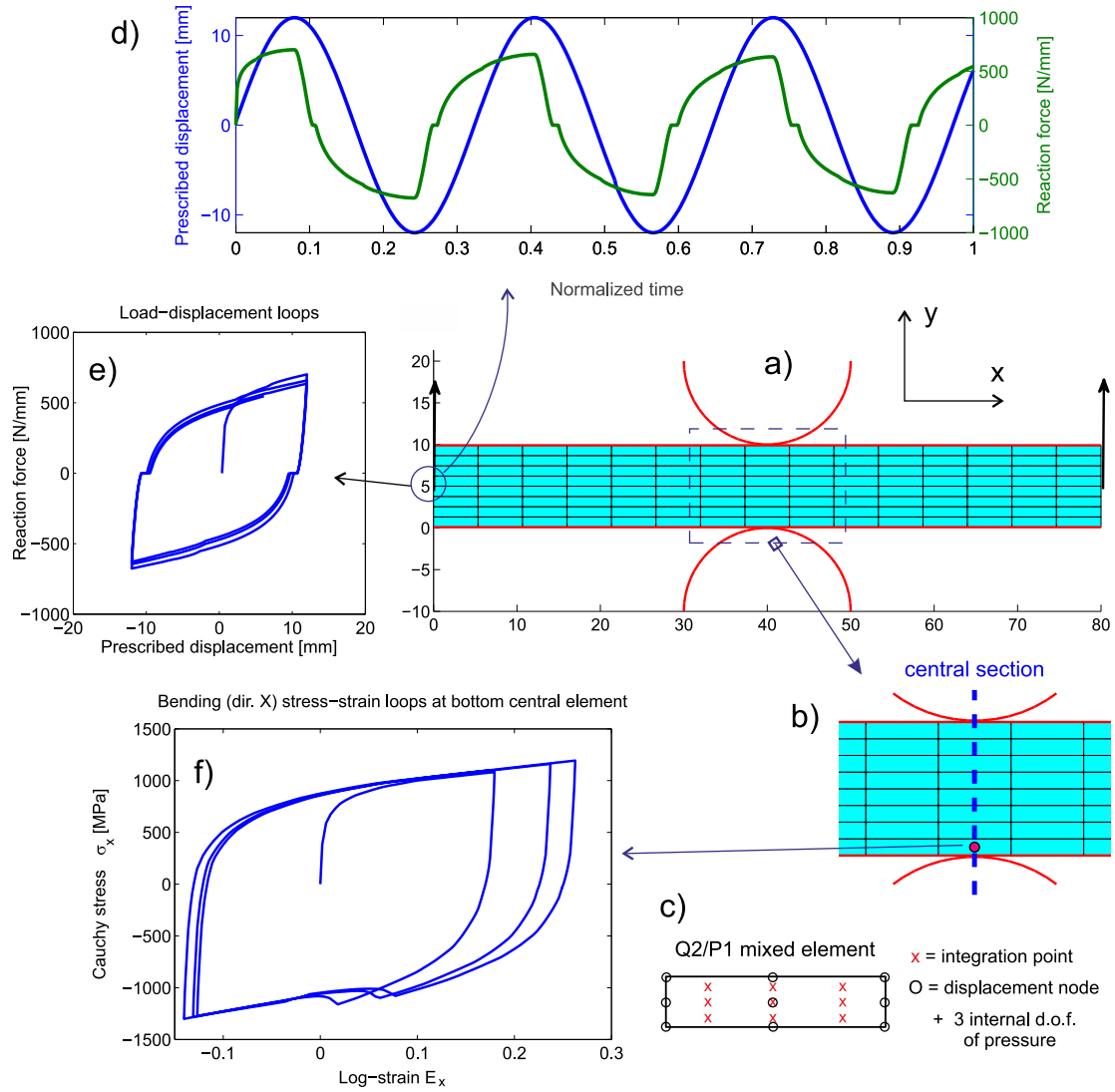


Figure 3: Cyclic bending of a  $80 \times 10 \text{ mm}^2$  plate (plane strain) using rollers of radius  $10 \text{ mm}$ . Plots (a), (b) detail the finite element mesh using a Q2/P1 mixed formulation (c). Plot (d) is the prescribed displacement of  $u = 12 \times \sin(bt) \text{ mm}$  and the resultant reaction force. Plot (e) shows the force-displacement cycles (note that due to plastic deformation there is a discontinuity). Figure (f) shows the stress-strain cycles near the lower roller. Note that in compression the kink is due to the contact with the lower roller. Reproduced from [20], under permission.

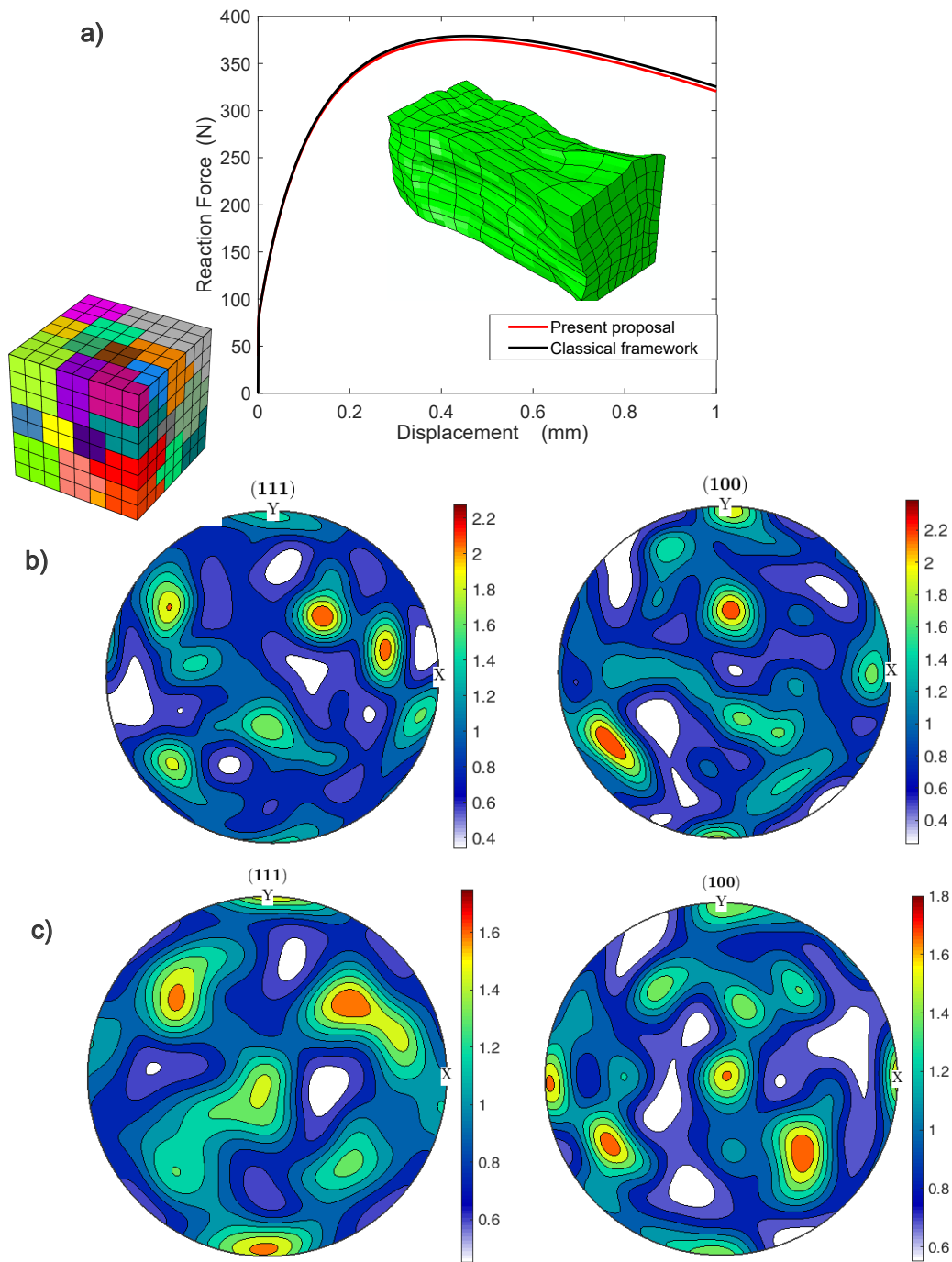


Figure 4: Simulation of the tensile test on a polycrystal sample with random texture. (a) Undeformed cubic specimen, load displacement curve also compared to the classical formulation, and deformed specimen. (b) Pole plots of the initial crystallographic texture for directions (111) and (100). (c) Pole plots of the final crystallographic texture for directions (111) and (100). Adapted from results in [21]; under permission.

## Acknowledgements



This work has received funding from the European Union's Horizon 2020 research and innovation programme under the Marie Skłodowska-Curie Grant Agreement No. 101007815

## References

- [1] K.J. Bathe, "Finite Element Procedures", Prentice Hall, USA, 1996, 2nd edition [K.J. Bathe], Watertown, MA, USA, 2014; also published by Higher Education Press, China, 2016.
- [2] K.J. Bathe, E. Ramm, E.L. Wilson, "Finite Element Formulations for Large Deformation Dynamic Analysis", *International Journal for Numerical Methods in Engineering*, 9(2), 353-386, 1975.
- [3] L.R.G. Treloar, "The Physics of Rubber Elasticity", Oxford University Press, Oxford, 1975.
- [4] R.W. Ogden, "Non-Linear Elastic Deformations", E. Horwood, New York, 1984.
- [5] J.C. Simo, T.J.R. Hughes, "Computational Inelasticity", Springer, New York, 1998.
- [6] T. Sussman, K.J. Bathe, "A Model of Incompressible Isotropic Hyperelastic Material Behavior Using Spline Interpolations of Tension-Compression Test Data". *Communications in Numerical Methods in Engineering*, 25(1), 53-63, 2009.
- [7] M. Latorre, F.J. Montáns, "Extension of the Sussman-Bathe Spline-Based Hyperelastic Model to Incompressible Transversely Isotropic Materials". *Computers and Structures*, 122, 13-26, 2013.
- [8] J. Crespo, M. Latorre, F.J. Montáns, "WYPIWYG hyperelasticity for isotropic, compressible materials". *Computational Mechanics* 59, 73-92, 2014.
- [9] M. Latorre, M. Mohammadkhah, C.K. Simms, F.J. Montáns, "A Continuum Model for Tension-Compression Asymmetry in Skeletal Muscle". *Journal of the Mechanical Behavior of Biomedical Materials*, 77, 455-460, 2018.
- [10] M. Latorre, E. Peña, F.J. Montáns, "Determination and Finite Element Validation of the WYPIWYG Strain Energy of Superficial Fascia from Experimental Data". *Annals of Biomedical Engineering*, 45, 799-810, 2017.
- [11] X. Romero, M. Latorre, F.J. Montáns, "The Relevance of Transverse Deformation Effects in Modeling Soft Biological Tissues", *International Journal of Solids and Structures*, 99, 57-70, 2016.
- [12] E. De Rosa, M. Laorre, F.J. Montans, "Capturing Anisotropic Constitutive Models with WYPIWYG Hyperelasticity, and on Consistency with the Infinitesimal Theory at sll Deformation Levels". *International Journal of Non-Linear Mechanics*, 96, 75-92, 2017.
- [13] V.J. Amores, K. Nguyen, F.J. Montáns, "On the Network Orientational Affinity Assumption in Polymers and the Micro-Macro Connection through the Chain Stretch". *Journal of the Mechanics and Physics of Solids*, 148, 104279, 2021.

- [14] V.J. Amores, J.M. Benítez, F.J. Montáns, “Data-driven, Structure-Based Hyperelastic Manifolds. A Macro-Micro-Macro approach to Reverse Engineer the Chain Behavior and Perform Efficient Simulations of Polymers”, *Computers and Structures* 231, 106209, 2020.
- [15] M. Latorre, F.J. Montáns, “A New Class of Plastic Flow Evolution Equations for Anisotropic Multiplicative Elastoplasticity based on the Notion of a Corrector Elastic Strain Rate”, *Applied Mathematical Modelling*, 55, 716-740, 2018.
- [16] M.A. Sáenz, F.J. Montáns, M. Latorre, “Computational Anisotropic Hardening Multiplicative Elastoplasticity based on the Corrector Elastic Logarithmic Strain Rate”, *Computer Methods in Applied Mechanics and Engineering*, 320, 82-121, 2017.
- [17] M. Latorre, F.J. Montáns, “Anisotropic Finite Strain Viscoelasticity Based in the Sidoroff Multiplicative Decomposition and Logarithmic Strains”, *Computational Mechanics*, 56, 503-531, 2015.
- [18] M. Latorre, F.J. Montáns, “Fully Anisotropic Finite Strain Viscoelasticity Based on a Reverse Multiplicative Decomposition and Logarithmic Strains”, *Computers and Structures*, 163, 56-70, 2016.
- [19] M. Latorre, F.J. Montáns, “Strain-Level Dependent Nonequilibrium Anisotropic Viscoelasticity: Application to the Abdominal Muscle”, *Journal of Biomechanical Engineering*, 139(10):101007, 2017.
- [20] M. Zhang, F.J. Montáns, “A Simple Formulation for Large-Strain Cyclic Hyperelasto-plasticity using Elastic Correctors. Theory and Algorithmic Implementation”, *International Journal of Plasticity*, 113, 185-217, 2019.
- [21] M. Zhang, K. Nguyen, J. Segurado, F.J. Montáns, “A Multiplicative Finite Strain Crystal Plasticity Formulation Based on Additive Elastic Corrector Rates: Theory and Numerical Implementation”, *International Journal of Plasticity*, 137, 102899, 2021.
- [22] H. Xiao, O.T. Bruhns, A. Meyers, “Objective Stress Rates, Path-Dependence Properties and Non-Integrability Problems”, *Acta Mechanica* 176, 135-151, 2005.
- [23] M. Kojić, K.J. Bathe, “Studies of Finite Element Procedures—Stress Solution of a Closed Elastic Strain Path with Stretching and Shearing Using the Updated Lagrangean Jaumann Formulation”. *Computers and Structures* 26(1-2), 175-179, 1987.
- [24] M. Latorre, F.J. Montáns, “Experimental Data Reduction for Hyperelasticity”. *Computers and Structures* 232, 105919, 2020.
- [25] J. Crespo, F.J. Montáns, “Function-Refresh Algorithms for Determining the Stored Energy Density of Nonlinear Elastic Orthotropic Materials Directly from Experimental Data”, *International Journal of Non-Linear Mechanics*, 107, 16-33, 2018.
- [26] S. Kawabata, M Matsuda, K. Tei, H. Kawai, “Experimental Survey of the Strain Energy Density Function of Isoprene Rubber Vulcanizate”, *Macromolecules* 14(1), 154.162, 1981.
- [27] V.J. Amores, F.J. Montáns, E. Cueto, F. Chinesta, “Crossing Scales: Data-

Driven Determination of the Microscale Behavior of Polymers From Non-Homogeneous Tests at the Continuum-Scale”, *Frontiers in Materials*, 9:879614, 2022.

- [28] R.W. Ogden, G. Saccomandi, I. Sgura, “Fitting Hyperelastic Models to Experimental Data”, *Computational Mechanics*, 34, 484-502, 2004.
- [29] P. Steinmann, M. Hossain, G. Possart, “Hyperelastic Models for Rubber-like Materials: Consistent Tangent Operators and Suitability for Treloar’s Data”, *Archive of Applied Mechanics*, 82, 1183-1217, 2012.
- [30] C. Miehe, S. Goktepe, F Lulei, “A Micro-Macro Approach to Rubber-Like Materials—Part I: The Non-Affine Micro-Sphere Model of Rubber Elasticity”. *Journal of the Mechanics and Physics of Solids*, 52(11), 2617-2660, 2004.
- [31] G. Marckmann, E. Verron, “Comparison of Hyperelastic Models for Rubber-Like Materials”, *Rubber Chemistry and Technology*, 79(5), 835-858, 2006.
- [32] V. Amores, L. Moreno, J.M. Benítez, F.J. Montáns, “A Model for Rubber-Like Materials with Three Parameters Obtained from a Tensile Test”, *European journal of Mechanics A/Solids*, 100, 104931, 2023.
- [33] G. Weber, L. Anand, “Finite Deformation Constitutive Equation and a Time Integration Procedure for Isotropic Hyperelastic-Viscoplastic Solids”. *Computer Methods in Applied Mechanics and Engineering*, 79, 173-202, 1990.
- [34] A. Eterović, K.J. Bathe, “A Hyperelastic-Based Large Strain Elasto-Plastic Constitutive Formulation with Combined Isotropic Kinematic Hardening Using Logarithmic Stress and Strain Measures”, *International Journal for Numerical Methods in Engineering*, 30(6), 1099-1114, 1990.